Detection of Curvilinear Structures by Tensor Voting Applied to Fiber Characterization

Nataliya Strokina, Tatiana Kurakina, Tuomas Eerola, Lasse Lensu, and Heikki Kälviäinen

Machine Vision and Pattern Recognition Laboratory (MVPR)
Department of Mathematics and Physics
Faculty of Technology
Lappeenranta University of Technology (LUT)
P.O. Box 20, 53851 Lappeenranta, Finland
firstname.surname@lut.fi
http://www2.it.lut.fi/mvpr

Abstract. The paper presents a framework for the detection of curvilinear objects in images. Such objects are challenging to be described by a geometrical model, and although they appear in a number of applications, the problem of detecting curvilinear objects has drawn limited attention. The proposed approach starts with an edge detection algorithm after which the task of object detection becomes a problem of edge linking. A state-of-the-art local linking approach called tensor voting is used to estimate the edge point saliency describing the likelihood of a point belonging to a curve, and to extract the end points and junction points of these curves. After the tensor voting, the curves are grown from high-saliency seed points utilizing a linking method proposed in this paper. In the experimental part of the work, the method was systematically tested on pulp suspension images to characterize fibers based on their length and curl index. The fiber length was estimated with the accuracy of 71.5% and the fiber curvature with the accuracy of 70.7%.

Keywords: curvilinear structure segmentation, edge linking, machine vision, image processing and analysis, pulping, papermaking.

1 Introduction

Detection of curvilinear structures appears in a number of applications. For example, the detection has been applied to the segmentation of biomedical [14] and geophysical images [15], and to the road detection in aerial images [8]. In real life images, there are also objects such as cables and wires that are difficult to be described by a geometrical model or that do not belong to a well-defined classes such as *car* or *person*. With such objects, curvilinear structures can be used for the detection.

The application field driving this specific research is pulping and papermaking, in particular, fiber characterization in pulp suspensions (see Fig. 1). The automated analysis of suspension images enables in-line real-time monitoring

J.-K. Kämäräinen and M. Koskela (Eds.): SCIA 2013, LNCS 7944, pp. 22–33, 2013.
© Springer-Verlag Berlin Heidelberg 2013

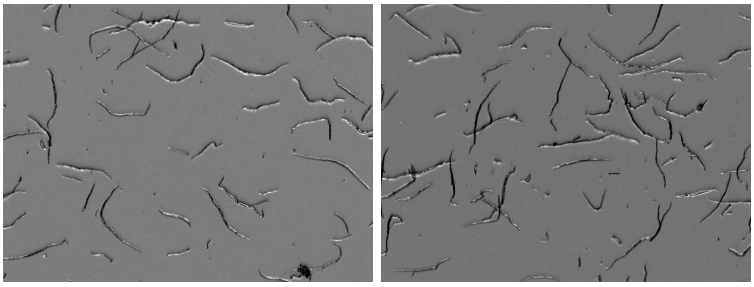

Fig. 1. Examples of the pulp suspension images. The image contrast has been increased for illustrative purposes.

and control for pulping and papermaking, and replaces the current off-line laboratory level analyses. Fiber properties, such as the length and the curl index, affect the formation of the paper web, and thus, it is important to monitor these properties during the papermaking process.

According to the review of Hirn and Bauer [5], there exist several commercial pulp/fiber analyzers such as FiberLab [3], MorFi [1], FS200 [3], and Fiber Quality Analyzer (FQA) [19]. These analyzers typically take a pulp sample and analyze it in laboratory conditions. This is time-consuming and does not allow real-time monitoring and control during the production. Some analyzers (e.g., FQA) incorporate a cytometric flow cell that orients and positions fibers for more precise measurements [19]. In the in-line measurements, however, it is impossible to orient the fibers which often create fiber bundles. On the contrary, it is important to estimate the percentage of fibers that are part of bundles.

A typical approach to implement the curvilinear structure detection is to detect salient points belonging to the structures followed by a grouping procedure [16]. In [7], curvilinear structures were recovered from the skeletons of grayscale images that were extracted by a distance transform utilizing edge maps of the images. In [6], the matched filter technique was applied to detect vessels segments in retinal images and an iterative threshold probing scheme was utilized to determine which pixels in the segments belong to vessels. The matched filter technique convolves an image with multiple filters that are designed to detect desirable features. In [4], spatial context in solar images was modelled with Markov Random Fields (MRF) extracting salient contours. The MRF based approaches applied to contour completion, such as [12], assign initial labels to salient points, formulate a cost function based on the label, and optimize it by relabeling the pixels which provides the final solution.

The proposed framework is based on tensor voting presented by Medioni et al. in [11]. In tensor voting, each pixel is associated with a tensor encoding the pixel orientation or the most probable orientation of a curve in that pixel. After an initialization, pixels cast votes in their neighborhood, described by a voting field, iteratively increasing the saliency of their neighbors belonging to the same curve. As a result of this voting, a saliency map is obtained, and it indicates the probability of pixels to belong to the curvilinear structures. Additionally, the

tensor voting provides pixel junction and polarity maps, showing which pixels belong to the junctions and which to the end points. The main advantage of the approach is that there is no need to optimize an explicitly defined complicated objective function.

The main contribution of this work is a formal description of a general framework for curvilinear structure detection, including a novel linking method. The second contribution is the application of the framework to the fiber detection and characterization.

The paper is organized as follows: Section 2 introduces the framework for the curvilinear structure detection utilizing the tensor voting approach. The experimental evaluation of the approach in terms of the fiber detection accuracy and the fiber length estimation is described in Section 3. The conclusions are given in Section 4.

2 Framework for Curvilinear Structure Detection

The curvilinear objects are recovered using the framework introduced in Fig. 2. A grayscale image is reduced to an edge map by an edge detection method based on direction sensitive filtering. Next, the tensor voting is applied to the edge map to retrieve the point saliency, end points, and junction points. Finally, the curves are grown from the most salient points utilizing the linking algorithm proposed in this paper.

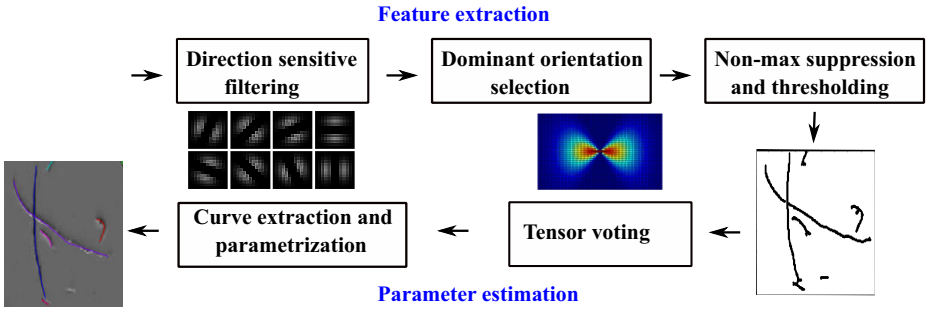

Fig. 2. Framework for curve extraction and parameterization

2.1 Oriented Edge Map Computation

To compute the edge map, an image is filtered by a second derivative zero-mean Gaussian filter in eight directions with the filter masks shown in Fig. 2. The dominant orientation of the edge normal in each pixel is computed as the maximum of the eight filter responses [9]. Non-maximum suppression in the dominant orientation of the edge normals is performed together with hysteresis thresholding as described in [2]. This procedure produces an oriented edge map where for each pixel p an orientation d is assigned.

2.2 Pixel Saliency Estimation

Saliency, in the context of curvilinear structure detection, indicates how likely it is that a pixel belongs to a curvilinear structure. To determine the saliency for each pixel, the tensor voting approach is applied. First, each pixel is associated with a tensor $\mathbf{T}$ that encodes the curve orientation of this pixel. The tensors are intialized as a matrix $\mathbf{T} = \begin{bmatrix} cos(d)^2 & cos(d)sin(d) \\ cos(d)sin(d) & sin(d)^2 \end{bmatrix}$ where d is a pixel orientation. After being initialized, each pixel votes for its neighbors in its voting field, supporting the assumption that they belong to the same curve. The voting field (see Fig. 3(a)) is oriented along the tangent to the curve in the pixel. It weights the pixels in the neighborhood, giving a higher weight to the pixels that are located along the curve. The size of the voting field $w \times w$ [10] is computed using a parameter σ, scale of voting, as

$$w = \frac{-16log(0.1) \cdot (\sigma - 1)}{\pi^2}. \tag{1}$$

The coefficient of the voting field in the pixel p is computed as

$$\mathbf{F}(l, \theta, \sigma) = e^{(-(\frac{s^2 + ck^2}{\sigma^2}))} \begin{bmatrix} -sin(2\theta) \\ cos(2\theta) \end{bmatrix} \begin{bmatrix} -sin(2\theta)\ cos(2\theta) \end{bmatrix} \tag{2}$$

where $s = \frac{\theta l}{sin(\theta)}$, $k = \frac{2sin(\theta)}{l}$, l is the distance to the voter, θ is the angle (see Fig. 3(b)), and c is a constant which controls the decay with high curvature. In the voting process, a voter's tensor is added to the tensors of the pixels in the voting field multiplied by the field coefficient. After the voting procedure, the saliency of a pixel is the difference between the bigger and the smaller eigenvalues of its tensor. The smaller eigenvalue indicates how likely it is that a pixel is a junction point. The whole process to obtain the saliency map is summarized in Algorithm 1.

2.3 Pixel Polarity Estimation

The previous step produces the saliency and junction point maps. To find the end points, information on the pixel polarity can be exploited [18]. A polarity vector indicates the direction where from the majority of the votes come. If most of the votes come from one direction, the point is likely to be an end point. Pixel polarity is computed as presented in Algorithm 2, using the first-order voting. Unlike in the second-order voting used in pixel saliency estimation, where the voting is done by matrices, in the first-order voting the votes are cast by vectors. A voter casts a vote to each pixel in its voting field as a vector oriented towards the voter (see Fig, 4(a)). As a result of voting, a polarity vector in each pixel is the sum of the vectors pointing to all the voters. Therefore, as illustrated in Fig. 4(b), polarity vectors of the end pixels are oriented towards the inner part of the curve. The polarity value is computed as the length of the polarity vector's projection on the vector tangent to the curve (perpendicular to the normal vector).

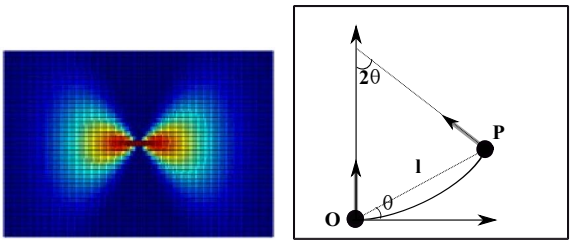

(a) (b)

Fig. 3. Voting field: (a) Example of a voting field oriented horizontally (the color corresponds to the field coefficient, with red representing a high and blue representing a low value); (b) Votes cast by a stick tensor located at the origin O; see the text for explanations of other symbols

Algorithm 1. Second-order tensor voting for edge saliency estimation.

Input: a set of edge pixels $\mathbf{P} = \{\mathbf{p_i} = [x_i, y_i, d_i]\}$ where the position of a pixel is described by its coordinates x_i, y_i and its orientation by angle d_i.
Output: a saliency map $\mathbf{S}$, a junction map $\mathbf{J}$.
Parameters: a scale of voting σ.

for each edge point $\mathbf{p_i}$ **do**
    Initialize the second order tensor as $\mathbf{T_i} = \begin{bmatrix} cos(d_i)^2 & cos(d_i)sin(d_i) \\ cos(d_i)sin(d_i) & sin(d_i)^2 \end{bmatrix}$.
end for
for each edge point $\mathbf{p_i}$ **do**
    Compute the tensor field coefficients $\mathbf{F_i}$ as in Eq. 2.
    Perform eigenvector decomposition of the tensor $\mathbf{T_i}$ to obtain eigenvalues ($\lambda 1_i$, $\lambda 2_i$) and eigenvectors ($\mathbf{e1}_i$, $\mathbf{e2}_i$).
    if $\lambda 1_i - \lambda 2_i > 0$ **then**
        for each edge point $\mathbf{p_j}$ in the voting field $\mathbf{F_i}$ **do**
            Compute a new tensor matrix $\mathbf{T_i} = \mathbf{T_j} + \mathbf{T_i}\mathbf{F_i}(\mathbf{p_j})$.
        end for
    end if
end for
for each edge point $\mathbf{p_i}$ **do**
    Perform eigenvector decomposition of the tensor $\mathbf{T_i}$ to obtain eigenvalues ($\lambda 1_i$, $\lambda 2_i$) and eigenvectors ($\mathbf{e1}_i$, $\mathbf{e2}_i$).
    Assign $\mathbf{S}(p_i) = \lambda 1_i - \lambda 2_i$ and $\mathbf{J}(p_i) = \lambda 2_i$.
end for

2.4 Curve Growing

The pixel saliency estimation and pixel polarity estimation steps produce the curve saliency, junction saliency, and end points maps. The final step is to extract the curvilinear structures from the image based on this information. For this, a curve gorwing method is used. According to [10], the curve growing starts by choosing an unprocessed seed point of high saliency and iteratively growing

Algorithm 2. First order tensor voting for polarity estimation.

Input: a set of edge pixels $\mathbf{P} = \{\mathbf{p_i} = [x_i, y_i, d_i]\}$ where x_i, y_i are the pixel coordinates and d_i its orientation.
Output: a polarity matrix $\mathbf{R}$.
Parameters: a scale of voting σ.

1: Initialize a polarity matrix $\mathbf{R}$ and a matrix of polarity vectors $\mathbf{P}$ by zero elements.
2: **for** each edge point $\mathbf{p_i}$ **do**
3: **for** each edge point $\mathbf{p_j}$ in a voting field of size w (Eq. 1) **do**
4: Compute a vector $\mathbf{t}$ oriented toward the edge point $\mathbf{p_i}$.
5: $\mathbf{P}(\mathbf{p_j}) = \mathbf{P}(\mathbf{p_j}) + \mathbf{t}$.
6: **end for**
7: **end for**
8: **for** each edge point $\mathbf{p_i}$ **do**
9: Compute $\mathbf{R}(\mathbf{p_i})$ as a length of the projection of vector $\mathbf{P}(\mathbf{p_i})$ on the tangent vector in the point $\mathbf{p_i}$.
10: **end for**

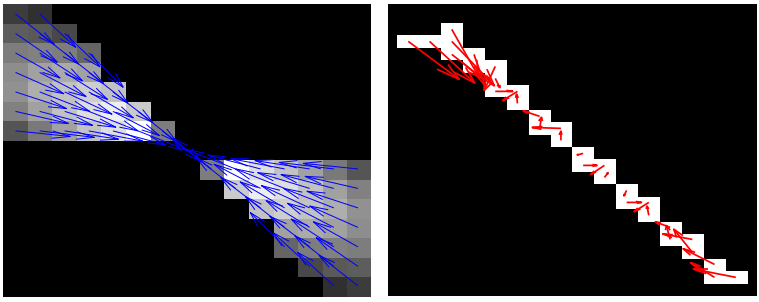

(a) (b)

Fig. 4. An example of the polarity map computation: (a) The polarity vectors generated by one voting pixel; (b) The map

the curve following the estimated tangent direction. A next point is added to the curve if it is a point with maximum saliency in the tangent direction. In [13], the importance of junction point and end point detection is emphasized and an approach for contour completion based on tensor voting is presented. However, the approach does not provide instructions for the separation of two or more intersecting curvilinear structures. In Algorithm 3, a method for curvilinear structure extraction is presented, where the curves are recovered as a set of pixels from the saliency map utilizing the information about the junction points and the polarity of the points. When the curve growing algorithm reaches a region of a junction selected by using a threshold T_j, the direction of growing stays as it was before the junction because in the junction region there is no certainty of the pixel orientation.

Algorithm 3. Curve extraction algorithm.

Input: a set of edge pixels $\mathbf{P} = \{\mathbf{p_i} = [x_i, y_i, d_i]\}$, where x_i, y_i are the pixel coordinates, d_i its orientation. a matrix of tensors $\mathbf{T}$, a polarity matrix $\mathbf{R}$, a saliency matrix $\mathbf{S}$, a junction matrix $\mathbf{J}$.
Output: a list of curves $\mathbf{Q} = \mathbf{q_m}$.
Parameters: a threshold for seed points selection $T1_s$, a saliency threshold $T2_s$, minimal polarity of an end point T_e, a threshold for junction points T_j.

Select a subset of seed points $\mathbf{P1} = \{\mathbf{p_i}\}$ with the saliency value $\mathbf{S_i} > T1_s$.
for all salient points $\mathbf{p_i}$ from the set **P1 do**
    Perform eigenvector decomposition of the tensor $\mathbf{T_i}$ to obtain eigenvalues ($\lambda 1_i$,$\lambda 2_i$) and eigenvectors ($\mathbf{e1_i}$, $\mathbf{e2_i}$).
    $\mathbf{q1}$ = CURVE_GROWING($\mathbf{S}$, $\mathbf{J}$, $\mathbf{R}$, $\mathbf{p_i}$, $\mathbf{e1}$).
    $\mathbf{q2}$ = CURVE_GROWING($\mathbf{S}$, $\mathbf{J}$, $\mathbf{R}$, $\mathbf{p_i}$, $-\mathbf{e1}$).
end for
Join two parts of the curve $\mathbf{q} = [\mathbf{q1}, \mathbf{q2}]$.
Add the curve to the list of the curves $\mathbf{Q} = [\mathbf{Q}, \mathbf{q}]$.

function CURVE_GROWING($\mathbf{S}$, $\mathbf{J}$, $\mathbf{R}$, $\mathbf{p}$, $\mathbf{e}$)
    Current seed point $\mathbf{p_{curr}} = \mathbf{p}$.
    while ($\mathbf{R}(p_{curr}) < T_e$) and ($\mathbf{S}(p_{curr}) < T2_s$) **do**
        $\mathbf{d_{curr}} = \mathbf{e}$.
        if $\mathbf{J}(\mathbf{p_{curr}}) > T_j$ **then**
            $\mathbf{d_{curr}} = \mathbf{d_{pred}}$.
        end if
        $\mathbf{p_{curr}}$ = the most salient point in the $\mathbf{d_{curr}}$ direction.
        Add $\mathbf{p_{curr}}$ to the curve $\mathbf{l}$.
        $\mathbf{d_{pred}} = \mathbf{d_{curr}}$.
    end while
    return l
end function

3 Experiments and Discussion

3.1 Data

The proposed approach to fiber detection and characterization was tested on a set of pulp suspension images, provided by the CEMIS-OULU Laboratory of the University of Oulu. The images were captured with a setup consisting of a CCD camera and optics with 2.5x magnification. The set consists of 50 grayscale acacia pulp suspension images with the resolution of 800x600 pixels. 40 randomly selected images (on the average 50 fibers per image) were used for testing and 10 images for learning the method parameters. Examples of the images are presented in Fig. 1. The results of fiber detection and characterization were evaluated based on the spatial ground truth (GT) data verified by an expert. As illustrated in Fig. 5(a), the end points and points of high curvature were marked for each fiber. Examples of the GT markings are presented in Fig. 5(b)

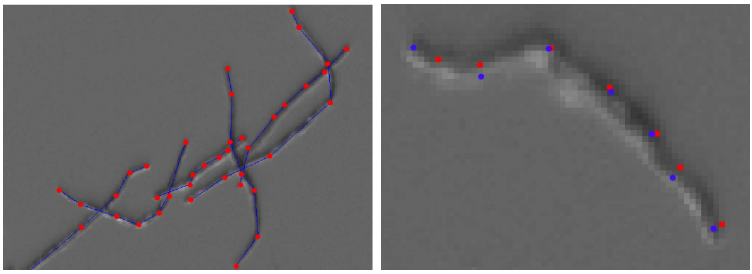

(a) (b)

Fig. 5. Examples of the ground truth markings. The colors are used only to illustrate separate fibers: (a) Illustration of the ground truth markings; (b) Ground truth fibers.

3.2 Experiments

The method parameters, presented in Table 1, were selected based on the method performance on 10 randomly selected suspension images. The scale of voting determines the size of the voting field and affects the size of gaps that are allowed in the curvilinear structures. The average length of fibers was 99 pixels. With the voting scale equal to 10, the biggest allowed gap is about 30 pixels. The thresholds for saliency, polarity, and junction maps affect the process of curve growing. The lower the saliency threshold, the longer the curve. The lower the polarity threshold, the sooner the growing is stopped. The junction threshold determines when the region of intersection starts.

Table 1. Method parameters

Parameter	Notation	Value
Scale of voting	σ	10
Saliency threshold for seed points selection	$T1_s$	50
Saliency threshold for curve growing termination	$T2_s$	10
Minimal polarity of end points	T_e	50
Threshold for junction points	T_j	40

Examples of the computed saliency map, junction map, and polarity map are presented in Fig. 6. The more prominent the pixel is, the brighter it is on the map. For example, the brighter pixels on the polarity map correspond to the pixels that are more likely to be end points.

Examples of detection results are presented in Fig. 7. While Figures 7(a) and 7(b) illustrate successful performance, Fig. 7(c) and 7(c) reveal difficulties. In Fig. 7(c), the fiber separation was performed incorrectly because of the small angle between the intersecting fibers. In Fig. 7(d), the algorithm failed because of the high number of intersecting fibers.

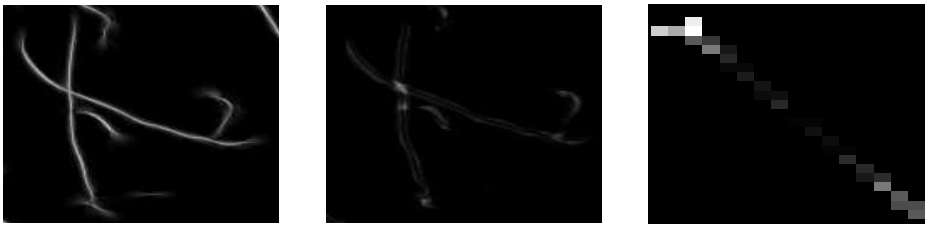

(a) (b) (c)

Fig. 6. Examples of saliency maps and polarity: (a) Saliency map; (b) Junction map; (c) Polarity map of a line segment

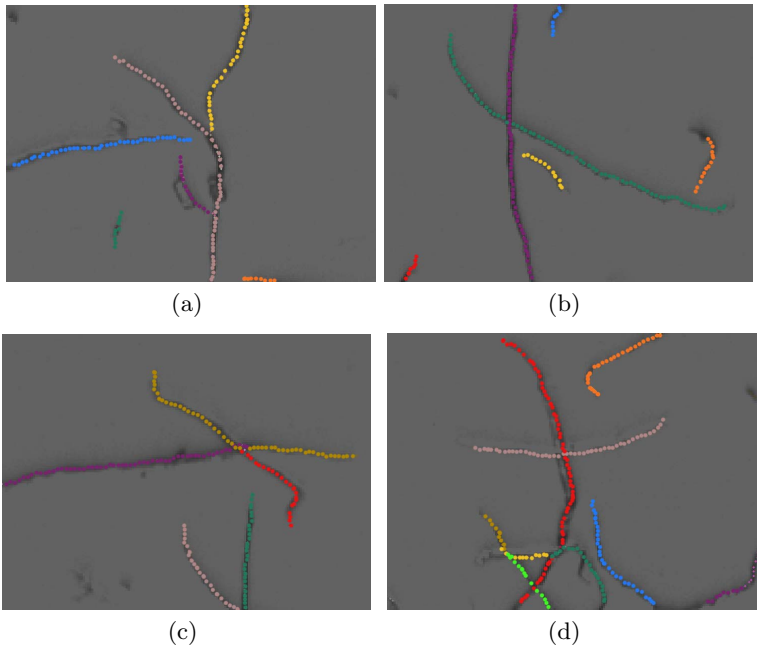

(a) (b) (c) (d)

Fig. 7. Examples of fiber detection. The colors are used only for illustrative purposes to visually separate the fibers.

To validate the detection results, for each GT fiber presented by a set of points $P_{gt} = \{p_1, ...p_N\}$, where N is the number points, we find a corresponding set $Q = \{(q_1, l_1), ..., (q_N, l_N)\}$, where q_i is the closest detected point for p_i and l_i is the label of a fiber the point q_i belongs to (see Fig. 5(b)). The detection error in pixels is computed as the average euclidean distance between the GT points and the corresponding (closest) detected points $E = \frac{1}{N}\sum_{i=1}^{N}(\|p_i - q_i\|)$. A fiber is detected correctly if $E < 6$. We distinguish the following detections:

- Percentage of correctly detected fibers (TP).
- Percentage of fibers that where fully detected but in several pieces (TP_M), where M is the number of pieces.
- Percentage of the detected fibers that are not even a part of a GT fiber (FP).

The results are shown in Fig. 8. 62% of the fibers were detected correctly in one piece. Moreover, 90% percent of fibers were fully detected in one or two pieces and almost all the fibers were fully detected in maximum of 4 pieces per fiber. The FP detection rate was 19.2% providing the precision of 80.8%. The average detection error E equalled to 3.8 pixels.

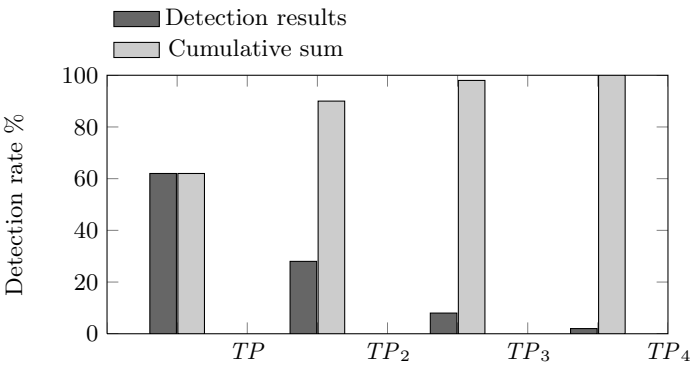

Fig. 8. Detection results

The length of a fiber presented by a sequence of pixels $\{(x_1, y_1), ..., (x_N, y_N)\}$ is computed as the sum of distances between the curve points [17] as

$$L = \sum_{i=2}^{N} \sqrt{(x_i - x_{i-1})^2 + (y_i - y_{i-1})^2}. \tag{3}$$

The projected length of a fiber is estimated as the distance between the curve end points [17] as

$$l = \sqrt{(x_n - x_1)^2 + (y_n - y_1)^2}. \tag{4}$$

The curl index [17] is calculated as the ratio between the full length and the projected length as

$$CI = \frac{L}{l} - 1. \tag{5}$$

The fiber parameters were computed as average values per image and the accuracy of the fiber parameter estimates was computed as the mean absolute error $(1 - \frac{P_{GT} - P}{P_{GT}}) \cdot 100\%$, where P_{GT} is a GT parameter value and P is a estimated parameter value. As the result, the fiber length was estimated with the accuracy of 71.5% and the fiber curl index with the accuracy of 70.7%.

4 Conclusion

A general framework for curvilinear structure detection including a novel linking method was presented. The framework was applied to fiber characterization in pulp suspension images. The method was shown to detect all the fibers in the set of used images but 38% of them in multiple pieces leading to a true-positive rate of 62%. The demonstrated precision of fiber detection was 80.8%. The average fiber length was estimated with the accuracy of 71.5% and the average fiber curvature with the accuracy of 70.7%. Problems occur when a single fiber is detected as several pieces causing false positive detections and the fiber parameter to be computed incorrectly. The future work will include further development of the curve growing algorithm and applying the framework to other similar problems.

Acknowledgements. The research was carried out in the "PulpVision" project (TEKES projects 70010/10 and 70040/11) funded by the European Union and the participating companies. The work was also supported by Finnish Foundation for Technology Promotion (TES). The authors wish to acknowledge Dr. Kaarina Prittinen and Kyösti Karttunen from the Measurement and Sensor Laboratory CEMIS-OULU from University of Oulu for providing data and expert knowledge.

References

1. Bartl, A., Pico, D.: Characterization of short fibers. In: The 9th International Conference on Chemical and Process Engineering (2009)
2. Canny, J.: A computational approach to edge detection. IEEE Transactions on Pattern Analysis and Machine Intelligence 8, 679–698 (1986)
3. Don, G., Sutherland, N., Rantanen, W.: Comparison of fiber length analyzers. In: Tappi Practical Papermaking Conference (2005)
4. Durak, N., Nasraoui, O.: Extracting salient contour groups from cluttered solar images via markov random fields. In: In Proceedings of the 18th IEEE International Conference on Image Processing (ICIP), pp. 2825–2828 (2011)
5. Hirn, U., Bauer, W.: A review of image analysis based methods to evaluate fiber properties. Lenzinger Berichte 86, 96–105 (2006)
6. Hoover, A.D., Kouznetsova, V., Goldbaum, M.: Locating blood vessels in retinal images by piecewise threshold probing of a matched filter response. IEEE Transactions on Medical Imaging 19(3), 203–210 (2000)
7. Jang, J.-H., Hong, K.-S.: Detection of curvilinear structures and reconstruction of their regions in gray-scale images. Pattern Recognition 35(4), 807–824 (2002)
8. Lin, Y., Saripalli, S.: Road detection from aerial imagery. In: The Proceedings of the IEEE International Conference on Robotics and Automation, pp. 3588–3593 (2012)
9. Lindeberg, T.: Edge detection and ridge detection with automatic scale selection. International Journal of Computer Vision 30, 117–154 (1998)
10. Medioni, G., Kang, S.: Emerging Topics in Computer Vision. Prentice Hall (2004)

11. Medioni, G., Lee, M., Tang, C.: A computational framework for segmentation and grouping. Elsevier (2000)
12. Ming, Y., Li, H., He, X.: Connected contours: A new contour completion model that respects the closure effect. In: The Proceedings of the IEEE Conference on Computer Vision and Pattern Recognition (CVPR), pp. 829–836 (2012)
13. Mordohai, P., Medioni, G.: Junction inference and classification for figure completion using tensor voting. In: Computer Vision and Pattern Recognition Workshop (2004)
14. Obara, B., Fricker, M., Gavaghan, D., Grau, V.: Contrast-independent curvilinear structure detection in biomedical images. IEEE Transactions on Image Processing 21(5), 2572–2581 (2012)
15. Panagiotakis, C., Kokinou, E., Sarris, A.: Curvilinear structure enhancement and detection in geophysical images. IEEE Transactions on Geoscience and Remote Sensing 49(6), 2040–2048 (2011)
16. Papari, G., Petkov, N.: Edge and line oriented contour detection: State of the art. Image and Vision Computing 29, 79–103 (2011)
17. Sutton, P., Joss, C., Crossely, B.: Factors affecting fiber characteristics in pulp. In: Pulping Process and Product Quality Conference Proceedings (2000)
18. Tong, W.-S., Tang, C.-K., Mordohai, P., Medioni, G.: First order augmentation to tensor voting for boundary inference and multiscale analysis in 3D. IEEE Transactions on Pattern Analysis and Machine Intelligence 26(5), 594–611 (2004)
19. Trepanier, R.: Automatic fiber length and shape measurement by image analysis. TAPPI Journal 81, 152–154 (1998)